Dark energy evolution and the curvature of the universe from recent observations

Kazuhide Ichikawa and Tomo Takahashi

Institute for Cosmic Ray Research, University of Tokyo, Kashiwa 277-8582, Japan

(Received 6 December 2005; published 27 April 2006)

We discuss the constraints on the time-varying equation of state for dark energy and the curvature of the universe using observations of type Ia supernovae from Riess *et al.* and the most recent Supernova Legacy Survey (SNLS), the baryon acoustic oscillation peak detected in the SDSS luminous red galaxy survey and cosmic microwave background. Because of the degeneracy among the parameters which describe the time dependence of the equation of state and the curvature of the universe, the constraints on them can be weakened when we try to constrain them simultaneously, in particular, when we use a single observational data. However, we show that we can obtain relatively severe constraints when we use all data sets from observations above even if we consider the time-varying equation of state and do not assume a flat universe. We also found that the combined data set favors a flat universe even if we consider the time variation of the dark energy equation of state.

DOI: 10.1103/PhysRevD.73.083526 PACS numbers: 95.36.+x, 98.80.−k

I. INTRODUCTION

Almost all current cosmological observations indicate that the present universe is accelerating. It can be explained by assuming that the universe is dominated by dark energy today. Although many candidates for dark energy have been proposed so far, we still do not know the nature yet. Many studies have been devoted to investigate dark energy assuming or constructing a specific model and then study its consequences on cosmological observations such as cosmic microwave background (CMB), large scale structure (LSS), type Ia supernovae (SNeIa), and so on. On the other hand, many efforts have also been made to study dark energy in a phenomenological way, i.e., as model independent as possible. In such approaches, dark energy can be parametrized with its equation of state and constraints on it can be obtained using cosmological observations. Assuming that the equation of state for dark energy w_X is constant in time, current observations give the constraint as $w_X \sim -1$ [1–6]. Although one of the most famous models for dark energy is the cosmological constant whose equation of state is $w_X = -1$, most models proposed so far have a time-varying equation of state. Thus, when we study dark energy, we should accommodate such time dependence in some way.

Many recent works on dark energy investigate the time dependence of the dark energy equation of state using simple parametrizations such as $w_X = w_0 + w_1(1 - a)$ with a being the scale factor of the universe [7,8]. Parametrizing the dark energy equation of state in such simple ways, the constraints on the time evolution of w_X have been considered in the literature (for recent works on this issue, for example, see Ref. [9]). It should be mentioned that, when one studies the equation of state for dark energy, it is usually assumed that the universe is flat. It should be also noted that dark energy is usually assumed to be the cosmological constant when one derives the constraint on the curvature of the universe. However, it has been discussed that, assuming a nonflat universe, the constraints on w_X and the curvature of the universe can be relaxed to some extent even with the time independent w_X from the CMB data alone [10]. Also, even if we assume a flat universe, there are degeneracies among the parameters which describe the evolution of dark energy, i.e., the time dependence of w_X when we consider the constraints on dark energy [11,12]. Furthermore, it has been also discussed that, if we remove the prior of a flat universe, the degeneracies becomes much worse [13]. Since it is very important to study the time dependence of w_X to differentiate the models of dark energy and also the curvature of the universe to test the inflationary paradigm, we should investigate how the prior on the curvature of the universe affects the determination of the time-varying equation of state for dark energy and vice versa. Some works along this line have been done using a specific one-parameter parametrization for the time-varying w_X [14].

In this paper, we study this issue, namely, the determination of the evolution of dark energy and the curvature of the universe, in some detail using the widely used parametrization of the equation of state for dark energy. We consider the constraints from observations of SNeIa reported in Refs. [4,6], the baryon acoustic oscillation detected in the SDSS luminous red galaxy survey [15], and recent CMB observations including WMAP [1]. In the next section, we summarize the analysis method we adopt in this paper. Then we discuss the constraints from the above-mentioned observations on the curvature of the universe with a time-varying equation of state for dark energy followed by the analysis on w_X without assuming a flat universe. The final section is devoted to the summary of the paper.

II. METHOD

In this section, we briefly summarize the method for constraining the parameters which describe the dark energy evolutions and other cosmological parameters. To study the evolution of dark energy, we use the following parametrization for the time-varying equation of state [7,8]:

$$w_X(z) = w_0 + \frac{z}{1+z} w_1 = w_0 + (1-a) w_1, \qquad (1)$$

where z is the redshift. In this parametrization, the equation of state at the present time is $w_X(z=0) = w_0$ and for the early time it becomes $w_X(z=\infty) = w_0 + w_1$. Since we are interested in the late-time acceleration of the universe due to dark energy, we consider the case where the dark energy dominates the universe only at late times. Thus, in this paper, we assume

$$w_0 + w_1 < 0, \qquad (2)$$

in order not to include the possibilities of early-time dark energy domination. With this parametrization, the energy density of dark energy can be written as

$$\rho_X(z) = \rho_{X0}(1+z)^{3(1+w_0+w_1)} \exp\left(\frac{-3w_1 z}{1+z}\right), \qquad (3)$$

where ρ_{X0} is the energy density of dark energy at present time. The Hubble parameter is given by

$$H^2(z) = H_0^2\bigg[\Omega_r(1+z)^4 + \Omega_m(1+z)^3 + \Omega_k(1+z)^2 + \Omega_X(1+z)^{3(1+w_0+w_1)} \exp\left(\frac{-3w_1 z}{1+z}\right)\bigg], \qquad (4)$$

where H_0 is the Hubble parameter at the present epoch, Ω_i is the energy density of a component i normalized by the critical energy density, and the subscripts r, m, k, and X represent radiation, matter, the curvature of the universe, and dark energy, respectively. To consider the constraints on dark energy and other cosmological parameters, we use the data from SNeIa, the baryon acoustic oscillation peak, and the CMB.

As for SNeIa data, we use the gold data set given in Ref. [4] and the first year data of the Supernova Legacy Survey (SNLS) released recently [6]. Constraints from SNeIa can be obtained by fitting the distance modulus which is defined as

$$M - m = 5\log\left(\frac{d_L}{\mathrm{Mpc}}\right) + 25. \qquad (5)$$

Here d_L is the luminosity distance which is written as

$$d_L = \frac{1+z}{\sqrt{|\Omega_k|}} \mathcal{S}\left(\sqrt{|\Omega_k|}\int_0^z \frac{dz'}{H(z')/H_0}\right), \qquad (6)$$

where $\mathcal{S}$ is defined as $\mathcal{S}(x) = \sin(x)$ for a closed universe, $\mathcal{S}(x) = \sinh(x)$ for an open universe, and $\mathcal{S}(x) = x$ with the factor $\sqrt{|\Omega_k|}$ being removed for a flat universe.

We also use the baryon acoustic oscillation peak detected in the SDSS luminous red galaxy survey [15]. To obtain the constraint, we make use of the parameter A which is defined as

$$A = \frac{\sqrt{\Omega_m}}{(H(z_1)/H_0)^{1/3}} \times \left[\frac{1}{z_1\sqrt{|\Omega_k|}}\mathcal{S}\left(\sqrt{|\Omega_k|}\int_0^{z_1}\frac{dz'}{H(z')/H_0}\right)\right]^{2/3}, \qquad (7)$$

where $z_1 = 0.35$ and A is measured to be $A = 0.469 \pm 0.017$ [15].

For the CMB data, we only use the shift parameter R which determines the whole shift of the CMB angular power spectrum [16]. R is given by

$$R = \frac{\sqrt{\Omega_m}}{\sqrt{|\Omega_k|}}\mathcal{S}\left(\sqrt{|\Omega_k|}\int_0^{z_2}\frac{dz'}{H(z')/H_0}\right), \qquad (8)$$

where $z_2 = 1089$. It has been discussed that using the CMB shift parameter is a robust way to include the constraints from observations of CMB [17]. From the recent observations of CMB including WMAP, CBI, and ACBAR, the shift parameter is constrained to be $R = 1.716 \pm 0.062$ [1,17].

In this paper, we only consider the effect of the modification of the background evolution by the change in the model and cosmological parameters. In fact, the properties of dark energy can also modify the evolutions of cosmic density fluctuation. When we consider the effects of dark energy perturbation, we also have to specify the speed of sound of the dark energy component. However, such modification can arise at the low multipole region of the CMB power spectrum where the errors due to cosmic variance are large. Thus, the constraints from CMB on dark energy mostly come from the position of acoustic peaks which can be described by the shift parameter. Hence, we do not consider the perturbation of dark energy in this paper.[1]

III. CONSTRAINTS ON THE Ω_m VS Ω_X PLANE

Now we discuss the implication of the dark energy evolution on the determination of the curvature of the universe. For this purpose, we derive the constraints from the observations on the Ω_m vs Ω_X plane. First, we consider the case with the constant equation of state for dark energy. In Fig. 1, we show the contours of 1σ and 2σ constraints from observations of SNeIa (a), the baryon acoustic oscillation peak (b), and the CMB shift parameter (c). We also show the constraint from the combination of all data sets (d). In Fig. 1, we assume the equation of state as $w_X = -1$. For the constraints from SNeIa, we used the gold data set from Ref. [4] and the data from SNLS [6] separately. As we can see, although each constraint from a single observa-

[1]However, the speed of sound can be useful to differentiate the models of dark energy. There are some works which discuss the constraint on the speed of sound. For interested readers, we refer them to Refs. [18–20].

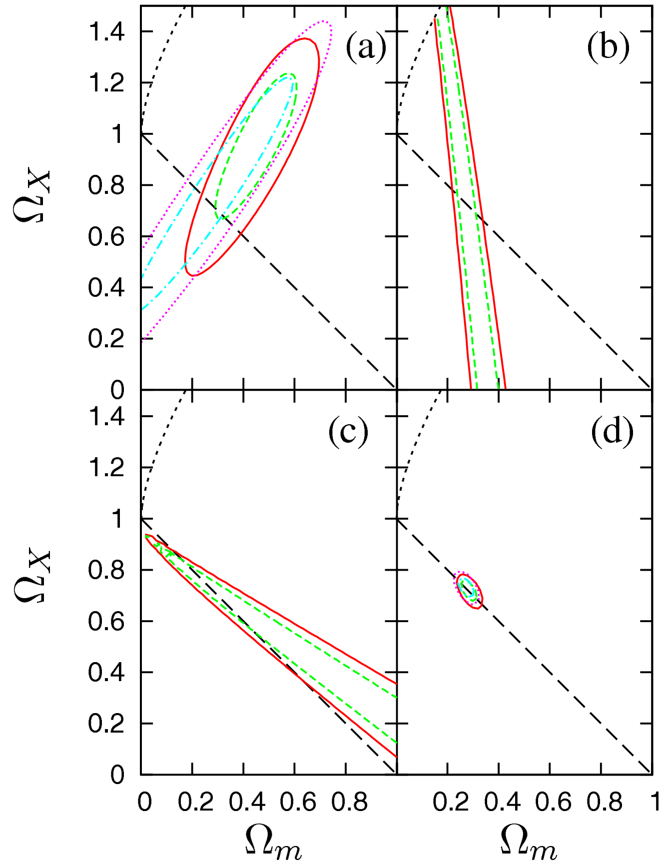

FIG. 1 (color online). Constraints on Ω_m and Ω_X from SNeIa (a), the baryon acoustic oscillation peak (b), the CMB shift parameter (c), and all data combined (d). For the constraint from SNeIa data and all data combined, we show the contours obtained from the gold set of Ref. [4] and SNLS [6] separately. Contours of 1σ (red solid line) and 2σ (green dashed line) are shown (for SNLS data, 1σ and 2σ contours are shown in the blue dash-dotted line and the purple dotted line, respectively). We assumed the cosmological constant as dark energy. The regions above the black dotted line are the parameter regions where there is no big bang singularity.

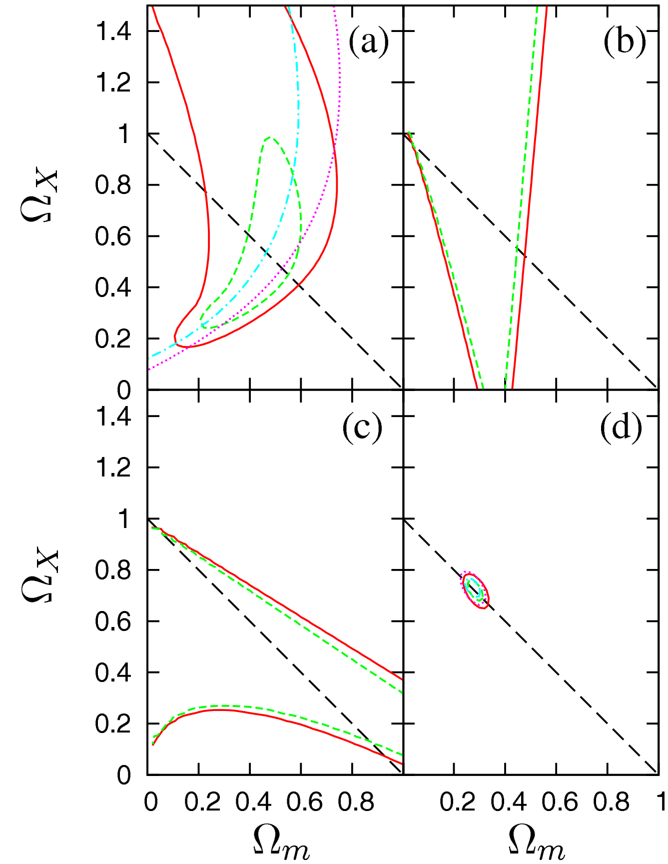

FIG. 2 (color online). The same as Fig. 1 except that we marginalized over the value of w_X. Here we considered the constant w_X.

tional data has the degeneracy in the Ω_m vs Ω_X plane, when all the data sets are combined, we can obtain a severe constraint as $\Omega_m \sim 0.3$ with $\Omega_k \sim 0$, which is a well-known result.

Next we consider the case where the equation of state for dark energy is allowed to vary, but still we keep w_X constant in time. In Fig. 2, we show the contours of 1σ and 2σ constraints after marginalizing over the values of w_X. Here we assumed the prior on w_X as $-5 \leq w_X \leq 0$. As seen from the figure, the allowed regions become larger compared to those for the case with fixing $w_X = -1$ when we use a single data set alone. However, by combining all data, we can obtain almost the same constraint as the case with $w_X = -1$ even though we marginalize over w_X. This result seems to be somewhat surprising at first sight. Thus we discuss the constraint more closely. In Fig. 3, the constraints on Ω_m and Ω_X for some fixed values of w_X are shown for each data set. As seen from the figure, we cannot find any region at which allowed regions of all three different observations overlap for the cases with $w_X = -0.7$ and -2. However, for the case with $w_X = -1$, constraints from all three data sets overlap around the region where $\Omega_m \sim 0.3$ and $\Omega_X \sim 0.7$. Also it should be noticed that the absolute minimum values of χ^2 from combined data sets for the cases with $w_X = -0.7$ and -2 are larger than that for $w_X = -1$ by $\chi^2_{\rm min}|_{w_X} - \chi^2_{\rm min}|_{w_X=-1} = 17.7$ and 58.7 for $w_X = -0.7$ and -2, respectively. This shows that the combination of all three data sets favors the case with $w_X = -1$ and the constraint on Ω_m and Ω_X becomes similar to the case with $w_X = -1$ being fixed even if we marginalize over w_X. In other words, this also means that, on marginalizing over w_X, each (Ω_m, Ω_X) requires different values of w_X for different observations except the region around $\Omega_m \sim 0.3$ with a flat universe where all three date sets favor $w_X \sim -1$. To see this, we plot contours of constant w_X which gives minimum values of χ^2 at each point on the Ω_m vs Ω_X plane in Fig. 4. We can clearly see that the favored values of w_X vary for different data sets except the region around $\Omega_m \sim 0.3$ with a flat universe. Observations we consider here measure some distance

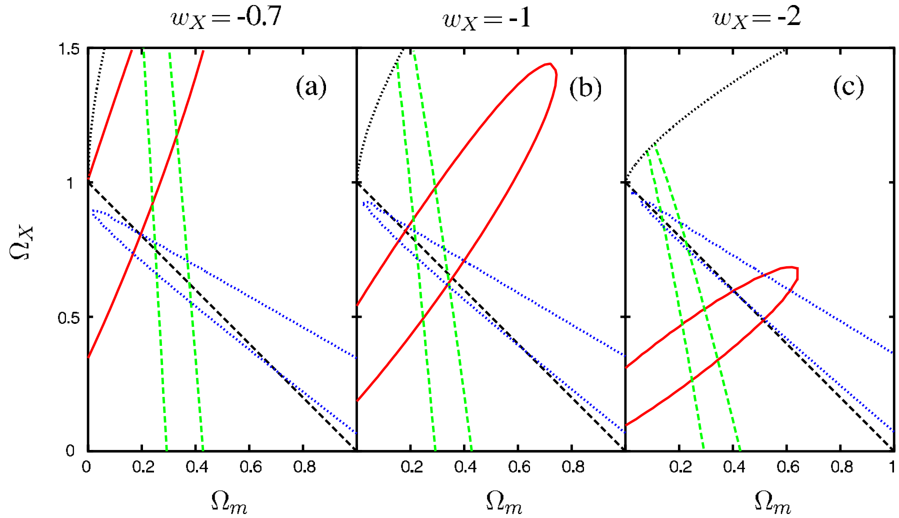

FIG. 3 (color online). Constraints on Ω_m and Ω_X for fixed values of the constant equation of state for dark energy from SNLS (red solid line), baryon acoustic oscillation (green dashed line) and CMB shift parameter (blue dotted line). The contours of 2σ constraint alone are shown in this figure. Here we take $w_X = -0.7$ (a), -1 (b), and -2 (c). The regions above the black dotted line are the parameter regions where there is no big bang.

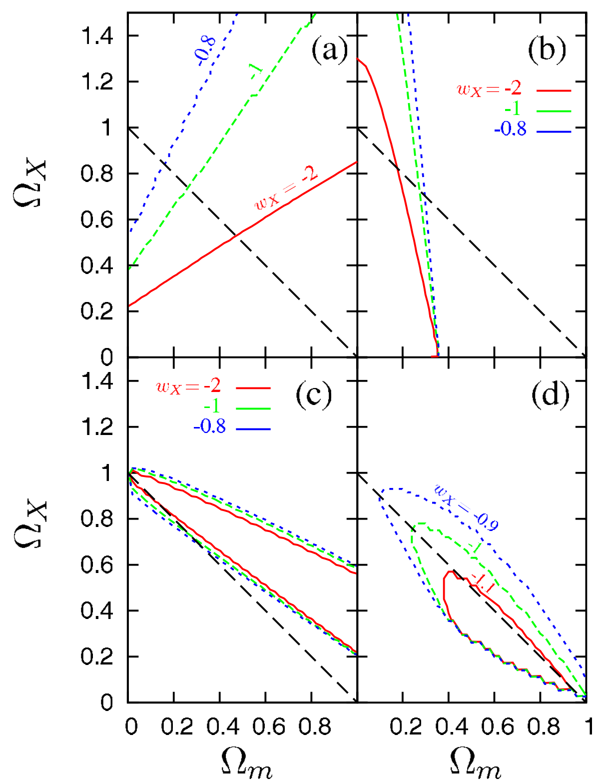

FIG. 4 (color online). Contours of constant w_X which gives minimum χ^2 when we marginalize over w_X for the constraints from SNeIa (a), the baryon acoustic oscillation peak (b), the CMB shift parameter (c), and all data combined (d). Contours of $w_X = -2$ (red solid line), -1 (green dashed line), and -0.8 (blue dotted line) are shown except for the case where all three data are combined [panel (d)]. For panel (d), contours of $w_X = -1.1$ (red solid line), -1 (green dashed line), and -0.9 (blue dotted line) are shown. For SNeIa, the data from SNLS are used here.

scales to certain redshifts which are determined by the energy density of matter Ω_m, dark energy Ω_X, and the equation of state w_X. If the value of w_X is not constrained to be -1, the density parameters Ω_m and Ω_X can have more freedom to be consistent with observations since the fit to the data depends on the combinations of these quantities. For a single observation, when w_X is allowed to vary, a larger range of (Ω_m, Ω_X) can be consistent with observations because of this degeneracy. However, when we use all observations, the combinations of Ω_m, Ω_X, and w_X which are consistent with observations become fairly limited. Thus, while the allowed regions become larger for each data set, when we combine all the data, the allowed region converges towards the concordance model with $\Omega_m + \Omega_X \sim 1$ and $\Omega_m \sim 0.3$ even if we do not assume the cosmological constant as dark energy.

Next we discuss the case with the time dependent equation of state parametrized as Eq. (1). As already pointed out in the literature, even if we assume a flat universe, there exists a degeneracy among the parameters which describe the evolution of equation of state for dark energy when we use a single observational data. It is also known that the degeneracy can be removed using more than one observation assuming the flatness. Here we discuss to what extent the evolution of dark energy equation of state can affect the determination of Ω_m and Ω_X when we do not assume a flat universe. In Fig. 5, the contours of 1σ and 2σ constraints are shown as the same manner as Fig. 1 except that we varied the values of both w_0 and w_1 which appear in Eq. (1) and marginalized over them to obtain the constraint. We assumed the prior on them as $-5 \leq w_0 \leq 0$ and $-4 \leq w_1 \leq 4$ under the condition of Eq. (2). For the constraint from SNeIa, the allowed regions get larger compared to the case with the constant equation of state discussed above

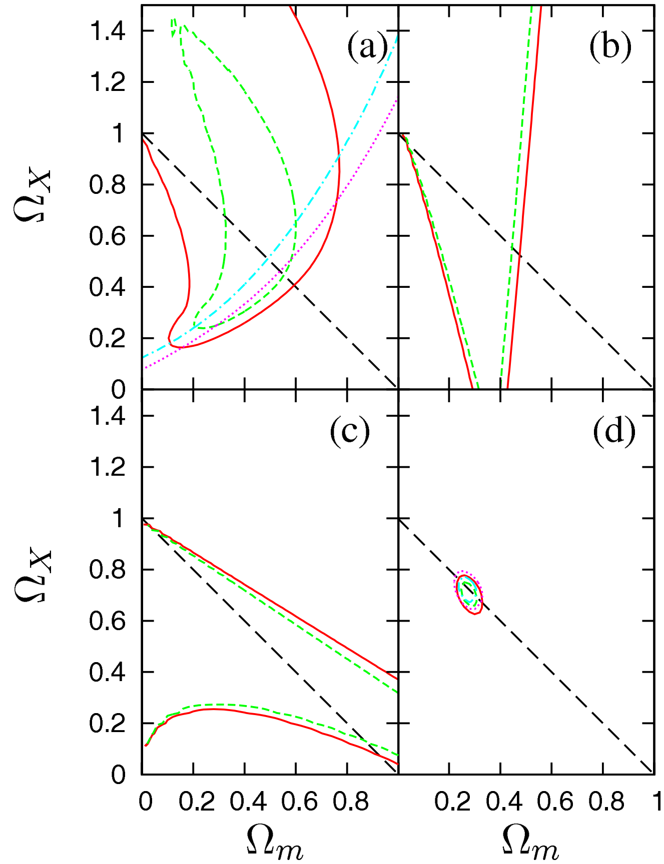

FIG. 5 (color online). The same as Fig. 1 except that we consider the time dependent equation of state for dark energy and marginalize over w_0 and w_1.

(see Fig. 2). As for the constraint from the baryon acoustic oscillation peak and the CMB shift parameter, the allowed regions are almost the same as the case with a constant equation of state. For observations which measure a single distance scale, the fit to the data does not significantly become better, even if the time evolution of w_X is allowed, due to the degeneracy between w_0 and w_1. Furthermore, when we use all three different observations together, the allowed region becomes almost the same as that of the case with a constant equation of state. This is because each observation favors different values of w_X. Even if we consider the time-varying equation of state, different combinations of w_0 and w_1 are chosen to minimize the value of χ^2 for each observation. Thus the allowed region from the combined data set is almost unchanged although the constraints from a single observation, in particular, from SNeIa, can become weaker.

Here we comment on the effect of the prior on w_0 and w_1. Although the constraints from a single data alone somewhat depend on the prior, the allowed region for all data combined is almost unaffected since the combinations of w_0 and w_1 favored around the allowed region from all data sets are far from the edge of the prior we assumed.

IV. CONSTRAINTS ON THE Ω_m VS w_X PLANE

In this section, we consider the constraints on the Ω_m vs w_X plane. First we show the constraint on Ω_m and w_0 in a flat universe with the equation of state for dark energy being constant. In Fig. 6, contours of 1σ and 2σ constraints from observations of SNeIa (a), the baryon acoustic oscillation peak (b), the CMB shift parameter (c), and all data combined (d) are shown. As is well known, SNeIa and CMB are complementary for constraining dark energy, which can be seen from the figure. In addition, we can see that the constraint from the baryon acoustic oscillation peak is also complementary. Thus we can obtain a severe constraint using all three data sets.

Next we consider the case with the time-varying equation of state for dark energy. Here we discuss the case with a flat universe. In Fig. 7, the constraints on Ω_m and w_0 are shown marginalizing over w_1. When we marginalize the values of w_1, we assumed the prior on w_1 as $-4 \leq w_1 \leq 4$. Similarly to the situation where we constrain Ω_m and Ω_X discussed in the previous section, if we consider the time-varying equation of state for dark energy, the allowed region becomes larger when we use a single data set. However, when we consider all three data sets, we can obtain a relatively severe constraint. Although the allowed region of w_0 extends to larger values, Ω_m is constrained to be $\Omega_m \sim 0.3$ which is almost the same as the case with assuming a constant equation of state. This is because the values of w_1 favored by different data sets given Ω_m and w_0 are different. Thus the degeneracy is removed to some extent when we use all three data sets combined.

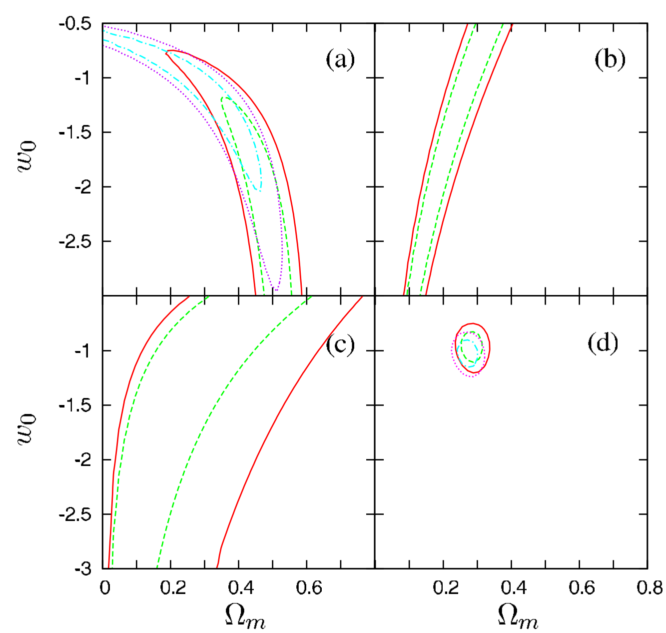

FIG. 6 (color online). Constraints on Ω_m and w_X from observations of SNeIa (a), the baryon acoustic oscillation peak (b), CMB (c), and all data combined (d). We assumed a flat universe and a constant equation of state here.

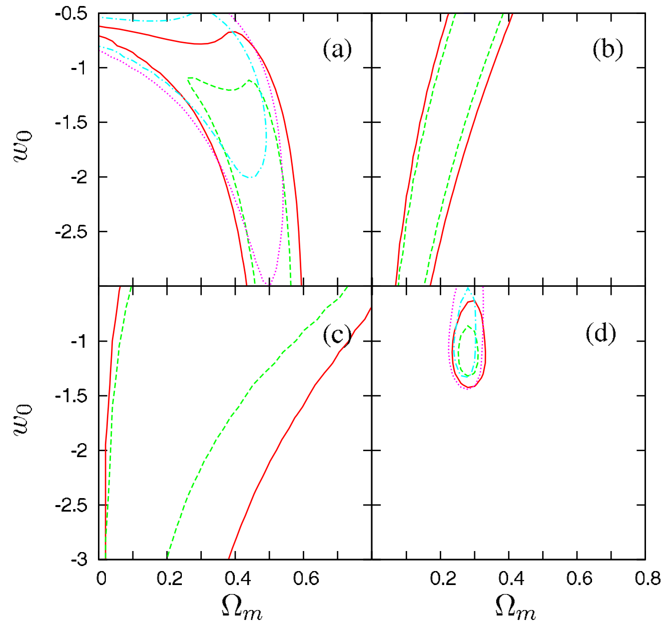

FIG. 7 (color online). The same as Fig. 6 except that we consider the time dependent equation of state for dark energy as in Eq. (1). To obtain the constraint, we marginalized over w_1. Here we assumed a flat universe.

Now we discuss the constraints without assuming a flat universe. First, we discuss the case with w_X being constant in time. In Fig. 8, we show the constraints from SNeIa (a), the baryon acoustic oscillation (b), and all data combined (c). For the last case, the data from the CMB shift parameter is included. To obtain the constraint, we marginalized over Ω_k with the prior $-0.3 \leq \Omega_k \leq 0.3$. Here we do not show the constraint from the CMB shift parameter alone since we cannot obtain a significant constraint from it in the parameter region we consider in Fig. 8. This is because, as it has already been pointed out, the curvature of the universe and w_X are strongly degenerate in the CMB power spectrum [10]. Again, although the constraints from a single data set alone are weakened, if we consider all data sets, we can obtain almost the same constraint as that with the case where a flat universe is assumed. Notice that the constraint on w_0 is also not changed much compared to that with flat universe prior. Hence, from Fig. 8 we can say that the prior on the curvature does not affect the determination of the equation of state for dark energy much.

We also show the case where we consider the time-varying equation of state without assuming a flat universe. In Fig. 9, the constraints are shown as the same as Fig. 8 except that we marginalized over both Ω_k and w_1 in this

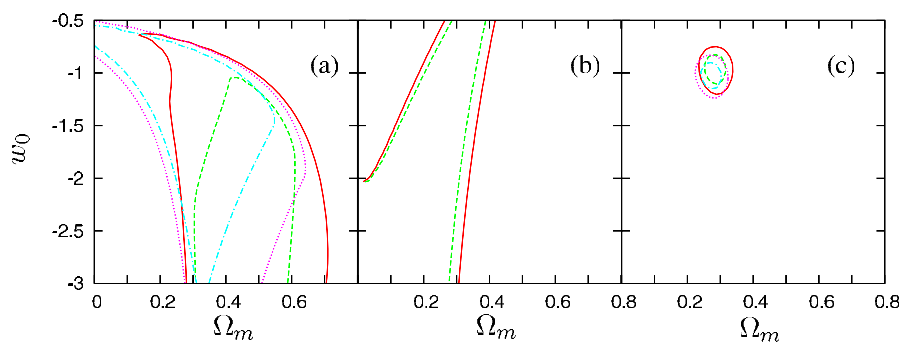

FIG. 8 (color online). Constraints on Ω_m and w_X from observations of SNeIa (a), the baryon oscillation (b), and all data combined (c). Here we do not assume a flat universe, but a constant equation of state for dark energy is assumed. In this figure, we marginalized over Ω_k.

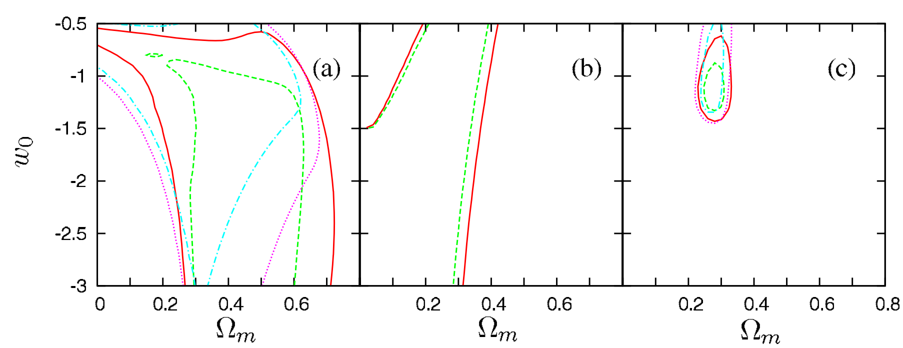

FIG. 9 (color online). The same as Fig. 8 except that we consider the time dependent equation of state for dark energy and do not assume a flat universe. In this figure, we marginalized over Ω_k and w_1.

case. The prior on w_1 is taken as $-4 \leq w_1 \leq 4$. The CMB shift parameter cannot give a significant constraint in the parameter range we consider in this case too. As in the previous cases, using each observational data alone, the allowed region becomes significantly larger compared to those with constant equation of state and a flat universe. However, when we use all data sets, the allowed region does not change much. From Figs. 6 and 8, we can conclude that the prior on the curvature of the universe does not affect the constraint on Ω_m and w_0 much if we use all data sets. In particular, we can obtain the constraint such that $\Omega_m \sim 0.3$ without assuming a flat universe. Moreover, the assumption of the constancy of the equation of state for dark energy also does not affect the constraint on Ω_m. When we consider the time-varying equation of state, the constraint on the equation of state becomes slightly weaker even if all data combined is used.

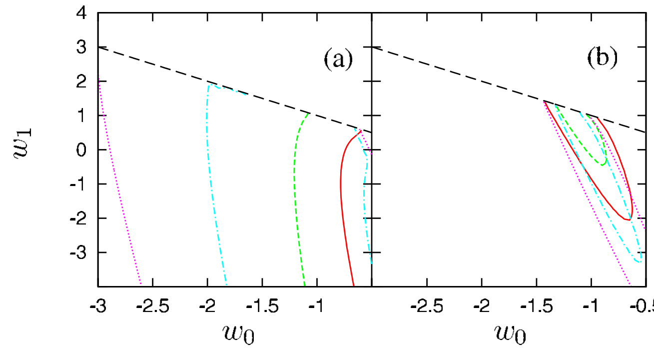

FIG. 11 (color online). Constraints on w_0 and w_1 from observations of SNeIa (a) and all data combined (b). A flat universe is assumed but we marginalized over Ω_m. We do not consider the region where $w_0 + w_1 > 0$ (the region above the dashed black line) not to include the possibilities of the early time domination of dark energy.

V. CONSTRAINTS ON THE EVOLUTION OF DARK ENERGY

In this section, we consider the constraints on the time dependence of dark energy equation of state, i.e., on w_0 and w_1 without assuming the prior of a flat universe. However, first we discuss the case with a flat universe for the later comparison with the case where a flat universe is not assumed. In Fig. 10, contours of 1σ and 2σ allowed regions are shown for the case with a flat universe. Here we fix the energy density of matter as $\Omega_m = 0.28$. Notice that we do not consider the region where $w_0 + w_1 > 0$ in order not to include the possibilities of early-time dark energy domination. As we can see from the figure, the constraint from SNeIa is stringent compared to baryon acoustic oscillation peak and CMB. Since the position of the baryon acoustic oscillation peak measures a single distance scale from $z = 0$ to $z = 0.35$ and the CMB shift parameter also gives a single scale from $z = 0$ to $z = 1089$, there is a strong degeneracy among the parameters which describe the equation of state for dark energy. Notice that the distance scales are determined by the integration of the inverse of the Hubble parameter, which can smear out the information on the time dependence of the equation of state. This is the reason why the strong degeneracy exists when only a single scale is considered. However, as for SNeIa data, the degeneracy is removed to some extent since we have the measure of the distance from $z = 0$ to various redshifts.[2] Thus observations of SNeIa can mainly constrain the time dependence of the equation of state for dark energy.

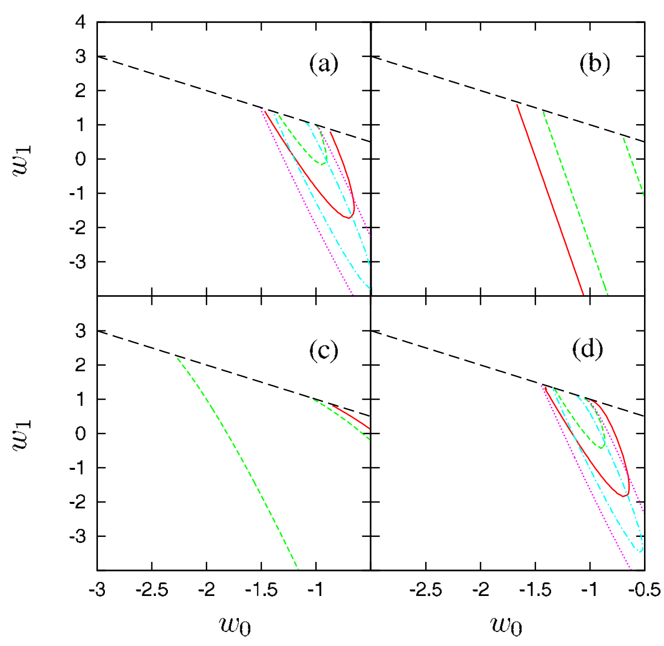

FIG. 10 (color online). Constraints on w_0 and w_1 from SNeIa (a), the baryon acoustic oscillation peak (b), the CMB shift parameter (c), and all data combined (d). We assumed $\Omega_m = 0.28$ with a flat universe. We do not consider the region where $w_0 + w_1 > 0$ (the region above the dashed black line) not to include the possibilities of the early time domination of dark energy.

Next we show the constraints on w_0 and w_1 in a flat universe without assuming a particular value for Ω_m. To obtain the constraint, we marginalized over Ω_m with the prior $0 \leq \Omega_m \leq 0.5$. In Fig. 11, we show the constraints on w_0 and w_1 from SNeIa (a) and all data combined (b). We do not show the constraints from the baryon acoustic oscillation peak and the CMB shift parameter each alone because we cannot obtain significant constraints from them in the parameter region of w_0 and w_1 we consider here. Also in this case, such severe degeneracies among the parameters exist because those observations measure a single distance scale. However, when we include all data sets in

[2] Of course, there is a limitation to determine the time dependence of the equation of state using current observations of SNeIa data [11,12].

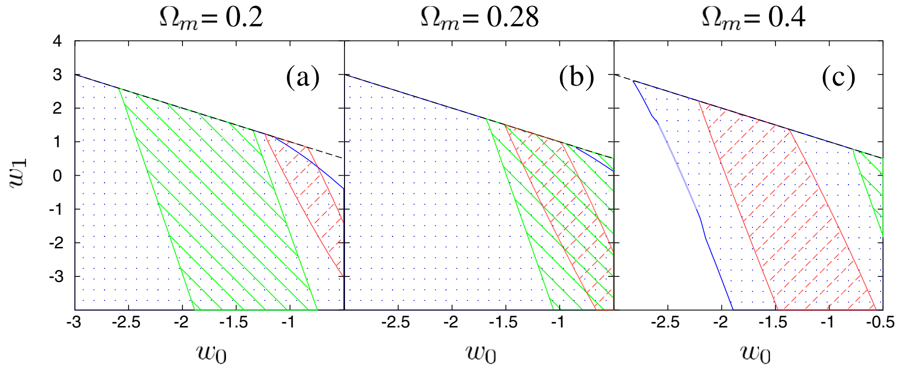

FIG. 12 (color online). 2σ constraints on w_0 and w_1 from observations of SNeIa (shaded with dashed red line), CMB (shaded with solid green line), and baryon acoustic oscillation (blue dotted region). The regions of 2σ constraint are shown here. The cases with $\Omega_m = 0.2$ (a), 0.28 (b), and 0.4 (c) are depicted. A flat universe is assumed in the figure.

the analysis, we can obtain almost the same constraint as that with Ω_m being fixed to 0.28. This is partly because the best fit value of Ω_m is near 0.28 when we marginalized over it, but also because the values of Ω_m minimizing χ^2 for each observational data set are different. For reference, we show the contours of allowed regions from each observation fixing the value of Ω_m in Fig. 12. In the figure, the cases with $\Omega_m = 0.2$, 0.28, and 0.4 are shown. As seen from the figure, all three allowed regions from different observations overlap at some region only in the case with $\Omega_m = 0.28$. In other cases, each observation favors different regions in the w_0 vs w_1 plane, which means that the combinations of different observations do not favor such values of Ω_m. Furthermore, it should be also mentioned that the minimum values of χ^2 for each case are different. Of course, the case with $\Omega_m = 0.28$ gives the smallest $\chi^2_{\rm min}$. For the other cases, the values of $\chi^2_{\rm min}$ become larger as $\chi^2_{\rm min}|_{\Omega_m} - \chi^2_{\rm min}|_{\Omega_m=0.28} = 14.7$ and 28.0 for the cases with $\Omega_m = 0.2$ and 0.4, respectively. To see this point more in a general manner, in Fig. 13, we show contours of constant Ω_m which minimize χ^2 when we marginalize over Ω_m for the constraints from SNeIa (a), the baryon acoustic oscillation peak (b), the CMB shift parameter (c), and all data combined (d). As is clear from the figure, preferred values of Ω_m for each observation are quite different. Thus when all data are used, we can obtain a severe constraint although a single observation cannot constrain the equation of state for dark energy much. It should be also mentioned that the prior on Ω_m does not affect the constraint on the time dependence of the equation of state when we use all data combined.

Now we discuss the case with Ω_m not being fixed and not assuming a flat universe. In Fig. 14, the allowed regions

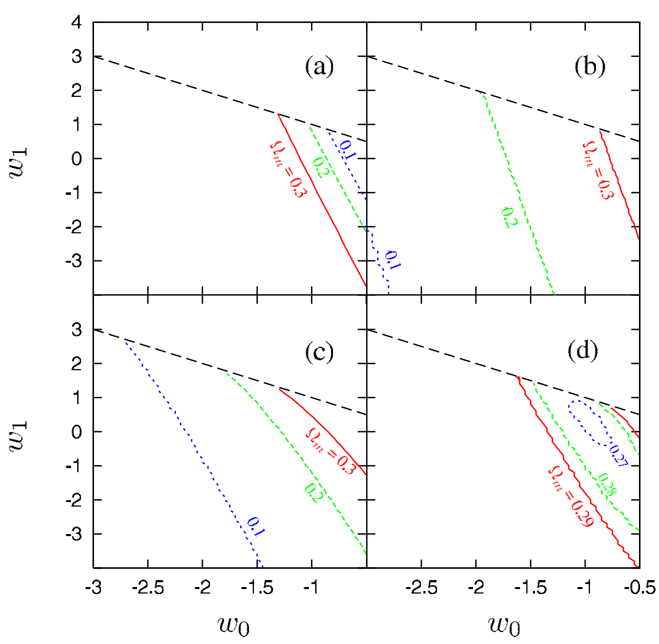

FIG. 13 (color online). Contours of constant Ω_m which gives minimum χ^2 when we marginalize over Ω_m for the constraints from SNeIa (a), the baryon acoustic oscillation peak (b), CMB shift parameter (c), and all data combined (d). Contours of $\Omega_m =$ 0.3 (red solid line), 0.2 (green dashed line), and 0.1 (blue dotted line) are shown except for the case where all three data are combined [panel (d)]. For panel (d), $\Omega_m = 0.29$ (red solid line), 0.28 (green dashed line), and 0.27 (blue dotted line) are shown. For SNeIa, we use the data from SNLS.

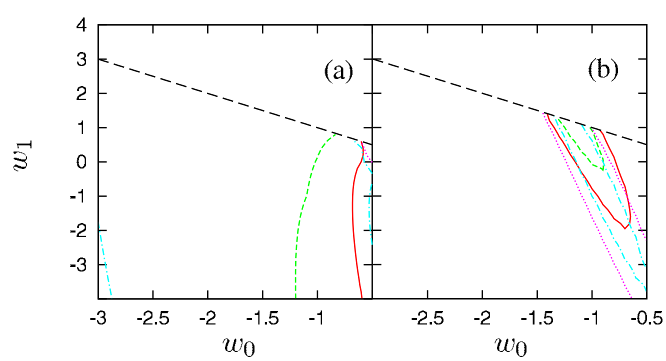

FIG. 14 (color online). The same as Fig. 11 except that we marginalized over Ω_m and Ω_k.

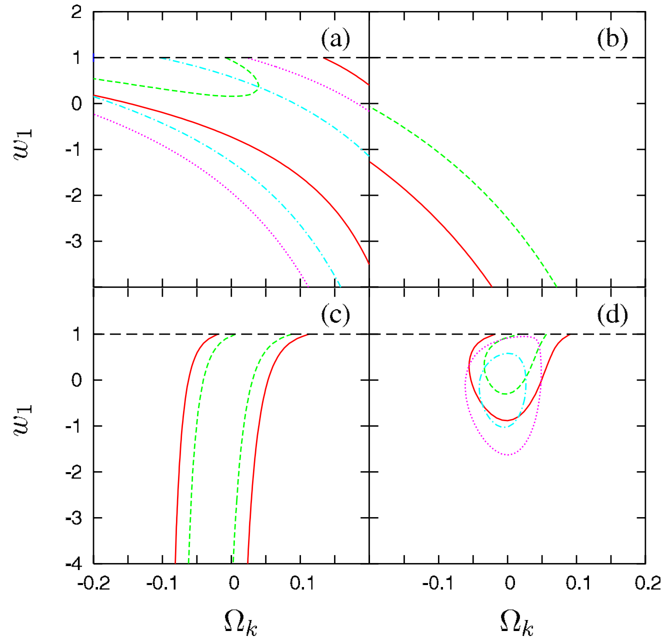

FIG. 15 (color online). Constraints on w_1 and Ω_k from SNeIa (a), the baryon acoustic oscillation peak (b), the CMB shift parameter (c), and all data combined (d). We fixed the other parameters as $\Omega_m = 0.28$ and $w_0 = -1$.

are shown after marginalizing over Ω_m and Ω_k. We assumed the prior on these variables as $0 \leq \Omega_m \leq 0.5$ and $-0.3 \leq \Omega_k \leq 0.3$. In this case, the constraint is significantly weakened when we consider a single data set alone. We only report here the constraint from SNeIa (a) and that from all data combined (b) since the baryon acoustic oscillation peak and the CMB shift parameter cannot give meaningful constraints on this plane in this case too. As we can see, when we consider the constraint from all data sets, it significantly becomes severe compared to that from SNeIa alone as seen from the figure. This is because the favored values of Ω_m and Ω_k from each data set are different as in the previous cases. Thus we can conclude that the prior on the curvature does not affect much the determination of the equation of state for dark energy if we use all data combined.

VI. CONSTRAINTS ON THE Ω_k VS w_1 PLANE

In this section, we discuss the constraints on the Ω_k vs w_1 plane, which has not been discussed much in the literature so far. In fact, the results that we are going to present in this section are essentially the reinterpretation of the results shown in the previous sections. In particular, as we have shown in Sec. III, we have already found that a flat universe is favored even if we consider the dark energy with a time-varying equation of state. [Notice that the contours of the constraints from all observational data lie around the line $\Omega_m + \Omega_X = 1$ in Figure 5(d)]. However, by investigating the problem from another point of view, we can expect that we obtain more insight on the determination of the dark energy evolution and the curvature of the universe.

In Fig. 15, we show the constraints on Ω_k and w_1 fixing other parameters as $\Omega_m = 0.28$ and $w_0 = -1$. As discussed repeatedly in the previous sections, although the constraints on the parameters are not so severe for a single observational data, we can obtain relatively stringent constraints when we combine all data set. In Fig. 15(d), the constraint on w_1 is bounded from below, but this is just because we fix w_0 as $w_0 = -1$. If we also allow w_0 to vary, we can expect that the bound is relaxed due to the degeneracy among the evolution of dark energy.

Now we consider the constraints marginalizing over the values of Ω_m fixing w_0 or vice versa and also marginalizing over both w_0 and Ω_m. In Fig. 16, we show the 1σ and 2σ constraints on the Ω_k vs w_1 plane marginalizing over Ω_m fixing $w_0 = -1$ (a), marginalizing over w_0 fixing $\Omega_m = 0.28$ (b), and marginalizing both Ω_m and w_0 (c). In Fig. 16, we used all data sets combined to obtain 1σ and 2σ constraints. When we marginalize Ω_m and/or w_0, the priors on these parameters are assumed to be $0 \leq \Omega_m \leq 0.5$ and $-2 \leq w_0 \leq 0$ under the condition that Eq. (2) is being taken into account. As seen from this figure, a flat universe is favored even if we marginalized over other parameters. It should be mentioned that the values of w_1 are not so severely constrained if we also vary w_0 even when we use all data combined because of the degeneracy among

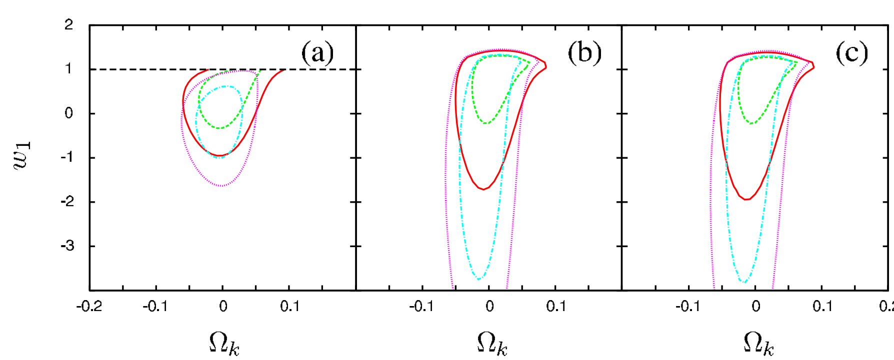

FIG. 16 (color online). Constraints on Ω_k and w_1 from all data combined for the cases with marginalizing over Ω_m with $w_0 = -1$ being fixed (a), marginalizing over w_0 with $\Omega_m = 0.28$ being fixed (b), and marginalizing over both Ω_m and w_0 (c).

the parameters describing the dark energy equation of state. We conclude this section by noting that current observations suggest that the flatness of the universe is quite robust irrespective of the nature of dark energy.

VII. SUMMARY

We considered the constraint on the curvature of the universe and the equation of state for dark energy from observations of SNeIa, the baryon acoustic oscillation peak, and the CMB shift parameter. Usually, when one discusses the curvature of the universe, dark energy is assumed to be the cosmological constant. Moreover, when one considers the constraint on the evolution of dark energy, in particular, the time dependence of the dark energy equation of state, a flat universe is usually assumed. In this paper, we discussed the constraints on the curvature of the universe without assuming the cosmological constant and also the time dependence of the equation of state for dark energy without assuming a flat universe. We showed that the constraint on the curvature of the universe is significantly relaxed from a single observation when we allow the time dependence in the dark energy equation of state. However, it was also shown that, when we use all data sets, the curvature of the universe or the energy density of matter and dark energy are severely constrained to be $\Omega_m \sim 0.3$ with a flat universe even if we consider the time-varying equation of state for dark energy. Observations we consider here measure some distance scales to certain redshifts which can be determined by the energy density of matter Ω_m, dark energy Ω_X, and the equation of state w_X. If we assume a broad range for w_X, the energy density of matter Ω_m and dark energy Ω_X can have more freedom to be consistent with observations since the fit to the data depends on the combinations of these variables. For a single observation, if w_X is allowed to vary more freely, much larger range of values of Ω_m and Ω_X can be consistent with observations. However, when we use all observations, the combinations of Ω_m, Ω_X, and w_X consistent with observations become fairly limited. Thus even if the allowed regions become large for each data set, when we combine all the data, we can obtain a severe constraint, which is interestingly almost the same region as what we obtain assuming the cosmological constant as dark energy.

We also investigated the constraint on the time-varying equation of state for dark energy without assuming a flat universe. Similarly to the situation where we constrained the curvature with the time-varying equation of state, the allowed region for w_X becomes larger when we use a single observational data. However, if we use all data sets considered in this paper, we can obtain almost the same constraint as that in the case where a flat universe is assumed.

Finally, we summarize what we found in this paper. The combination of the current observations:

(i) favors a flat universe regardless of the prior on the equation of state for dark energy with or without time evolution;

(ii) favors $\Omega_m \sim 0.3$ regardless of the flatness prior and the prior on the equation of state for dark energy with or without time evolution;

(iii) yields constraints on the time evolution of dark energy equation of state regardless of the prior on Ω_m and Ω_k.

In future observations, we can obtain much more stringent constraints on the equation of state for dark energy as well as the curvature of the universe regardless of the prior on other cosmological parameters. Hence we can expect that we will be able to have much insight on the nature of dark energy and also the inflationary paradigm.

ACKNOWLEDGMENTS

We are grateful to James Bjorken for valuable suggestions. T. T. would like to thank the Japan Society for Promotion of Science for financial support.

[1] D. N. Spergel *et al.*, Astrophys. J. Suppl. Ser. **148**, 175 (2003).
[2] M. Tegmark *et al.* (SDSS Collaboration), Phys. Rev. D **69**, 103501 (2004).
[3] J. L. Tonry *et al.* (Supernova Search Team Collaboration), Astrophys. J. **594**, 1 (2003).
[4] A. G. Riess *et al.* (Supernova Search Team Collaboration), Astrophys. J. **607**, 665 (2004).
[5] C. J. MacTavish *et al.*, astro-ph/0507503.
[6] P. Astier *et al.*, Astron. Astrophys. **447**, 31 (2006).
[7] M. Chevallier and D. Polarski, Int. J. Mod. Phys. D **10**, 213 (2001).
[8] E. V. Linder, Phys. Rev. Lett. **90**, 091301 (2003).
[9] Y. Wang and M. Tegmark, Phys. Rev. Lett. **92**, 241302 (2004); B. Feng, X. L. Wang, and X. M. Zhang, Phys. Lett. B **607**, 35 (2005); H. K. Jassal, J. S. Bagla, and T. Padmanabhan, Mon. Not. R. Astron. Soc. **356**, L11 (2005); D. A. Dicus and W. W. Repko, Phys. Rev. D **70**, 083527 (2004); S. Hannestad and E. Mortsell, J. Cosmol. Astropart. Phys. 09 (2004) 001; U. Seljak *et al.*, Phys. Rev. D **71**, 103515 (2005); F. Giovi, C. Baccigalupi, and F. Perrotta, Phys. Rev. D **71**, 103009 (2005); A. Upadhye, M. Ishak, and P. J. Steinhardt, Phys. Rev. D **72**, 063501 (2005); H. K. Jassal, J. S. Bagla, and T. Padmanabhan, Phys. Rev. D **72**, 103503 (2005); M. Doran, K. Karwan, and C. Wetterich, J. Cosmol. Astropart. Phys. 11 (2005) 007; S. Nesseris and L. Perivolaropoulos, Phys. Rev. D **72**, 123519 (2005); J. Q. Xia, G. B. Zhao, B. Feng, H. Li, and

X. Zhang, Phys. Rev. D **73**, 063521 (2006).

[10] J. L. Crooks, J. O. Dunn, P. H. Frampton, H. R. Norton, and T. Takahashi, Astropart. Phys. **20**, 361 (2003).

[11] I. Maor, R. Brustein, and P. J. Steinhardt, Phys. Rev. Lett. **86**, 6 (2001); **87**, 049901(E) (2001).

[12] I. Maor, R. Brustein, J. McMahon, and P. J. Steinhardt, Phys. Rev. D **65**, 123003 (2002).

[13] Y. Wang and M. Tegmark, in Ref. [9].

[14] Y. g. Gong and Y. Z. Zhang, Phys. Rev. D **72**, 043518 (2005).

[15] D. J. Eisenstein *et al.*, Astrophys. J. **633**, 560 (2005).

[16] J. R. Bond, G. Efstathiou, and M. Tegmark, Mon. Not. R. Astron. Soc. **291**, L33 (1997).

[17] Y. Wang and P. Mukherjee, Astrophys. J. **606**, 654 (2004).

[18] R. Bean and O. Dore, Phys. Rev. D **69**, 083503 (2004).

[19] J. Weller and A. M. Lewis, Mon. Not. R. Astron. Soc. **346**, 987 (2003).

[20] S. Hannestad, Phys. Rev. D **71**, 103519 (2005).